

Electronic Supplemental Information for:

**Overcoming confinement limited swelling in hydrogel thin films
using supramolecular interactions**

*Clinton G. Wiener, R.A. Weiss, Bryan D. Vogt**

Department of Polymer Engineering, University of Akron, Akron, OH 44325

* Email: vogt@uakron.edu (B.D.V.)

Part 1. Temperature correction of QCM-D data

This correction accounts for both the changes in the kinematic viscosity of water and the intrinsic characteristics of the quartz sensor / electronics with temperature. In general, this correction is most critical for ultrathin films, where the effects of temperature contribute significantly to the signal. For example if we consider the 10 nm thick (dry) film, nearly 50% of frequency shift measured with QCM-D can be attributed to temperature dependent changes in physical properties of the water and the characteristics of the quartz sensor. As both components of the correction are critical, we utilize a single correction that can account for both effects in a facile manner.

To determine the correction factor, the frequency change (ΔF) and dissipation change (ΔD) of clean sensors were measured in RO water as a function of temperature from 35 °C to 5 °C using a similar temperature step protocol as used for the hydrogel swelling experiments. These baseline measurements on the clean sensors were performed in triplicate to insure the observed shifts are

not artifacts, but a true measurement of the temperature dependencies. For each temperature, the correction factor is determined at equilibrium (defined as $\Delta F < 6$ Hz/h) for each overtone. These correction factors for ΔF and ΔD in water are fit as a function of temperature. Although both linear and quadratic fits provide similar statistics, the quadratic fit provides an improved physical representation of the temperature dependence due to two reasons. First, with the linear fit correction of the 10 nm thick (dry) NF5 film, there is an increase in the dissipation at high temperature that would not be physically expected in a collapsed film (Figure S1) as the difference in swelling between at 35 °C and 25 °C is quite small. Conversely, there is no substantial change in the dissipation when using the quadratic fit to correct the dissipation of the 10 nm thick (dry) NF5 film this same temperature range from 35 °C to 25 °C; this is the expected behavior.

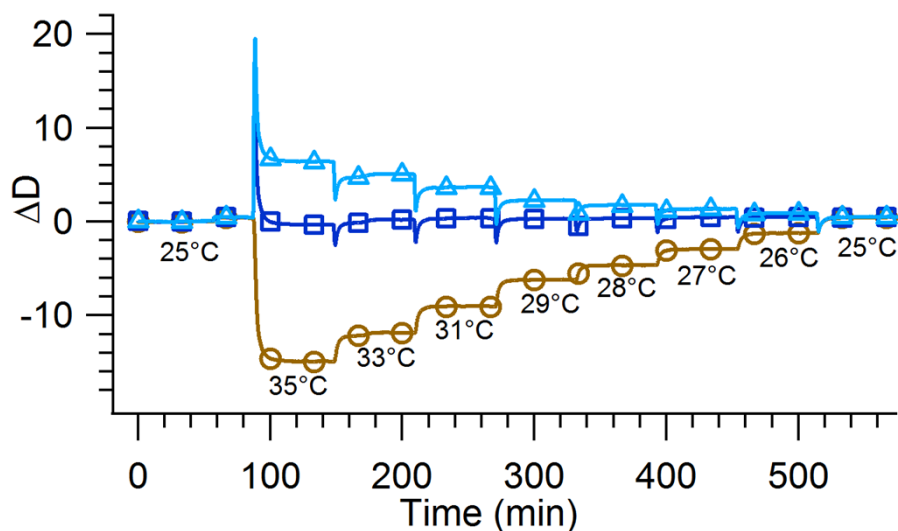


Figure S1. Dissipation curves for the 10 nm NF5 film at the start of a swelling run with temperatures for each step labeled. The three curves represent the 3rd overtone for: raw data (\ominus), with quadratic correction factor applied (\boxplus), and with linear correction factor applied (\boxminus). Note that the linear correction overcorrects the dissipation at high temperatures and implies a

non-physical result of increase dissipation upon collapse of the hydrogel when the temp is raised from 25 °C

A second reason for selection of the quadratic fit is the temperature dependence of the kinematic viscosity (ν) of water as shown in Figure S2, which is not linear. As both ΔF and ΔD of viscous fluids can be related to ν ,¹ this quadratic fit should provide an adequate form for the applied temperature correction if viscous effects are dominant. Using this quadratic expression, each overtone of the bare crystal in water is individually fit to develop a temperature correction factor to implement in the swelling experiments.

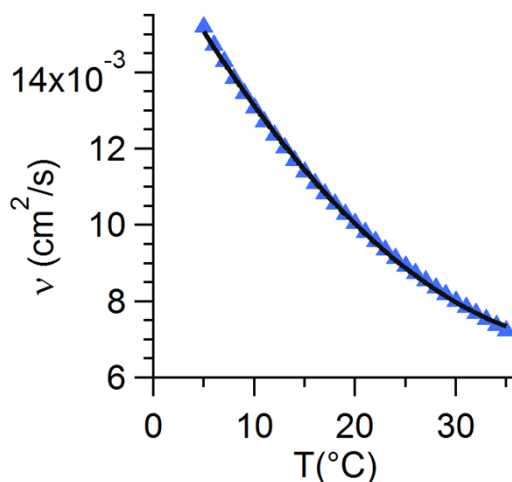


Figure S2. Kinematic viscosity, ν , (\blacktriangle) of water as a function of temperature (data obtained from NIST Chemistry WebBook)². Solid black provides a quadratic fit of the data.

Figure S3 shows the determined correction factor for the five overtones (overtones 3-11) for both the frequency and dissipation; these correction factors include both the temperature dependence of the kinematic viscosity of water and the intrinsic sensitivity of the crystal. In order to correct the data, this temperature dependent correction factor is subtracted from the raw

data for each overtone. The reference temperature is 25 °C (standard temperature for AT-cut crystals), so the correction is zero at 25 °C. Table S1 provides the temperature dependent parameters obtained for the five overtones, each with the quadratic expression: $\Delta F(T) = A_F T^2 + B_F T + C_F$, $\Delta D(T) = A_D T^2 + B_D T + C_D$. It should be noted that these parameters may also include some contributions specific to the electronics of the QCM-D, so these correction factors should ideally be determined for each QCM-D instrument.

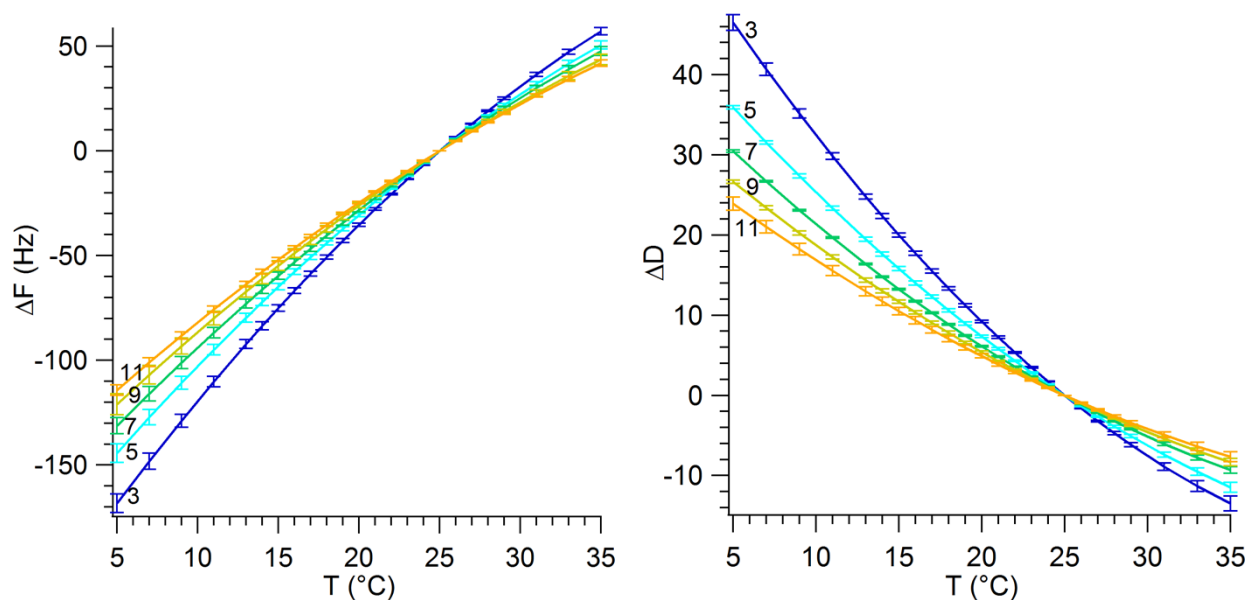


Figure S3. Overtone dependent temperature correction factors for ΔF and ΔD according to the best fit of a quadratic to a bare sensor in water. These changes are subtracted from the raw data to correct for all temperature dependencies in the system.

Table 1. The temperature correction parameters for the five overtones for both frequency and dissipation.

Overtone	Frequency			Dissipation		
	A_F	B_F	C_F	A_D	B_D	C_D
3	-0.0836	10.8	-215	0.0288	-3.18	61.4
5	-0.0635	8.97	-182	0.0239	-2.54	48.1
7	-0.0565	8.17	-166	0.0189	-2.10	40.5
9	-0.0502	7.46	-152	0.0165	-1.85	35.9
11	-0.0465	7.09	-145	0.0150	-1.67	32.2

To illustrate the impact of application of these temperature corrections, Figure S4 shows the difference in the film thickness using different models to fit the QCM-D data with and without this correction. At low temperatures in the highly swollen state, the Sauerbrey approximation for thickness is not strictly valid,³ but illustrates the overprediction of the swelling without the temperature correction as compared to the thicknesses determined from SE in Figure S4. More strikingly, fitting both the frequency and dissipation with the viscoelastic model shows an even greater difference between the corrected and uncorrected data. Without the temperature correction, the fit suggests a nearly linear increase in thickness with temperature using this standard viscoelastic model to describe the QCM-D data. With temperature correction, the swelling dependence on temperature is found to be sigmoid-like, which is consistent with the SE and bulk measurements.⁴ For the 32 nm film (shown in Figure S4), the temperature correction has a drastic effect on the thickness with nearly 30% reduction in calculated thickness at low temperatures (highly swollen) and 25% increase in calculated thickness at high temperatures (collapsed). In the collapsed state, both methods used to analyze the QCM-D data predict the same thickness when the temperature correction is applied (inset of Figure S4).

The temperature correction protocol results in improved agreement between the QCM-D and SE results for swelling of the thin films, especially when applying the viscoelastic model to fit

the QCM-D data. To our knowledge, there is no well-defined, standard protocol for temperature dependencies with QCM-D. These corrections are particularly important for the thinner films. This method of correction applies a simple offset that includes temperature effects associated with the QCM-D sensor and equipment, for which the temperature dependent physical properties of water alone cannot account. This correction also produces data that can easily be included in the standard Q-Tools program to fit the QCM-D data range.

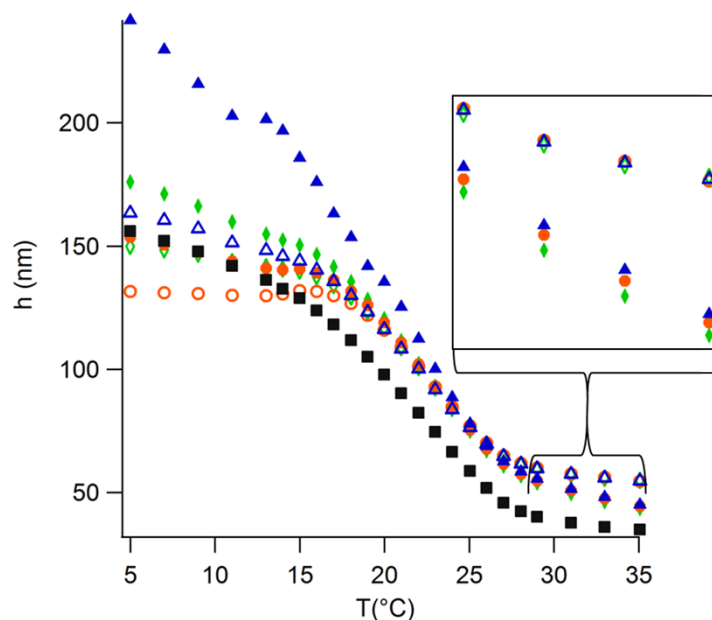


Figure S4. Influence of the correction on the temperature dependent thickness for a 32 nm (dry) NF5 film using the Sauerbrey approximation and viscoelastic modeling. **Solid symbols** represent the raw uncorrected data and **open symbols** are the temperature corrected data. Inset shows that after temperature correction, the Sauerbrey and viscoelastic modeled thicknesses converge in the high temperature limit. The overtones are determined by the Sauerbrey expression (3rd \blacklozenge , 5th \bullet) and viscoelastic model (\blacktriangle). For comparison, the thickness determined from SE (\blacksquare) is also included.

Part 2. LCST determination through Sigmoid curve fit

Following the prior work of Harmon et al.,⁵ the LCST was determined by fitting the swelling data to a sigmoid expression as shown in equation 1,

$$\frac{h}{h_0} = \left(\frac{h}{h_0} \right)_{\max} + \left[\frac{\left(\frac{h}{h_0} \right)_{\text{collapsed}} - \left(\frac{h}{h_0} \right)_{\max}}{1 + \exp\left(\frac{T_{LCST} - T}{\sigma} \right)} \right] \quad (1)$$

where $(h/h_0)_{\text{collapsed}}$ is the swelling ratio at high temperature (e.g., collapsed state), $(h/h_0)_{\max}$ is the swelling ratio at low temperature (e.g., highly swollen state), T_{LCST} is the inflection temperature that is denoted to be the LCST, and σ is the half width of the sigmoid, which provides a measure of the width of the LCST transition. Figure S5 shows how this parameterization fits the SE data for a 75 nm film with the parameters in equation 1 illustrated as well.

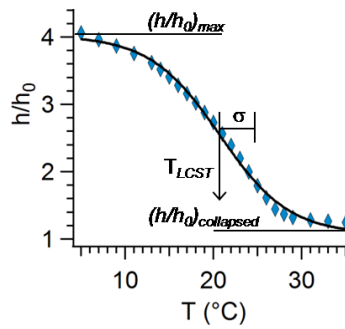


Figure S5: Sigmoid fit of SE data for 75 nm (dry) NF5 film. Thickness components $(h/h_0)_{\max}$ and $(h/h_0)_{\text{collapsed}}$ are associated with the swelling (vertical) axis, while the LCST and σ are associated with the temperature (horizontal) axis.

Part 3. Stress relaxation evidence from QCM-D and SE

Stress relaxation by physical domain rearrangement in the NF5 hydrogel is hypothesized to enable the swelling of the thin films to approach that of the bulk hydrogel. Careful examination of the swelling data as equilibrium is approached provides some indirect evidence for this rearrangement. Figure S6 illustrates the swelling behavior for a 120 nm film during a single temperature step from 25 °C to 24 °C. There are small jump-like increases in thickness and frequency after the initial swelling increase. These relatively large jumps may be indications of the rearrangement of the hydrophobic domains that could allow further swelling. Conversely, Figure S6 illustrates the swelling behavior for a 120 nm film during a single temperature step from 33 °C to 31 °C, where no overall increase in thickness occurs after the initial swelling. There are only slight fluctuations of 1 Å and 1 Hz in these data. This behavior would be consistent with no significant stress relaxation; the swelling at high temperatures is consistent with the constrained swelling predicted by Flory-Rehner, so this behavior would be expected.

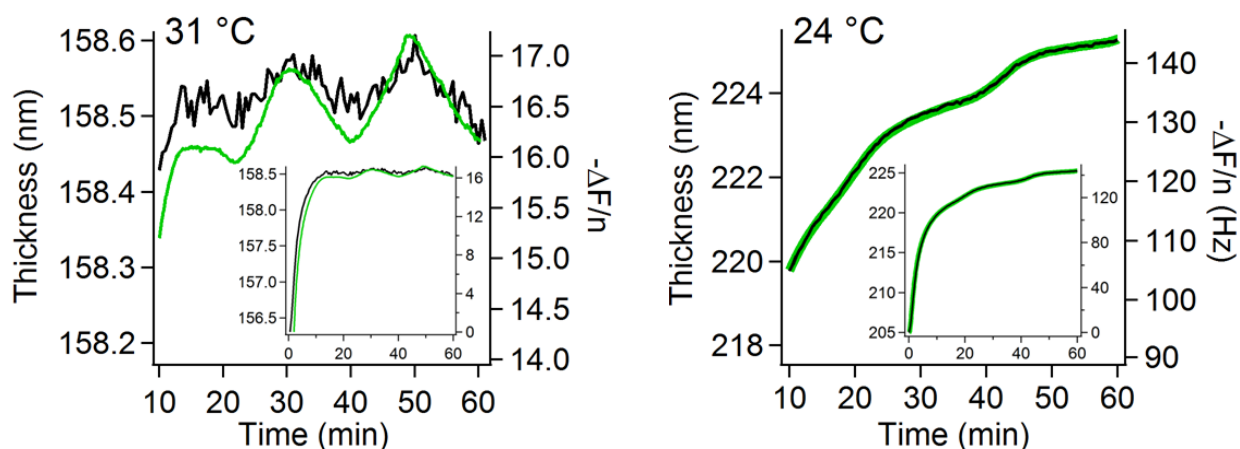


Figure S6. Swelling of 120 nm film as measured by QCM-D (thick green line) and SE (black line) for 33 °C to 31 °C and 25 °C to 24 °C temperature steps. The inset shows the swelling for the entire step.

Part 4. Determination of coupled water layer associated with QCM-D

For a single film thickness as shown in Figure S4, the offset between QCM-D and SE appears to be almost invariant with temperature with greater swelling reported by the QCM-D at all temperatures. This behavior is actually observed for all film thicknesses measured with the swelling from QCM-D being greater than that from SE (Figure 4). The average thickness difference between QCM-D and SE is 26 ± 12 nm. Prior reports have also observed a similar phenomenon associated with the thickness of adsorbed layers between QCM-D and optical techniques.⁶ This difference is generally attributed to coupled water at the surface that adds to the mass measured by QCM-D, but is not visible to SE. To understand if such a large coupled water layer (26 nm) might be present at the surface of the NF5 hydrogels, this thickness was subtracted from the thickness determined by VE fit of the QCM-D data with a direct comparison to the SE swelling as shown in Figure S7 for each film thickness from 32 to 120 nm. In general, the agreement between SE and QCM-D after this subtraction is good for temperatures greater than 18 °C. The behavior of the 75 nm film is different from the other films as the swelling is still overestimated by QCM-D at high temperatures. One explanation is that the film may have been rougher than the other film; this surface roughness could lead to additional coupling of water. However at low temperatures (<18 °C) for all films, the QCM-D thickness appears to be overcorrected with the swelling underestimated in comparison to the swelling measured by SE. This behavior suggests that the coupled water layer may be temperature dependent. However as this underestimation occurs in the highly swollen state, this difference could also be attributed to decreases in the surface roughness on swelling that would decrease the amount of coupled water.

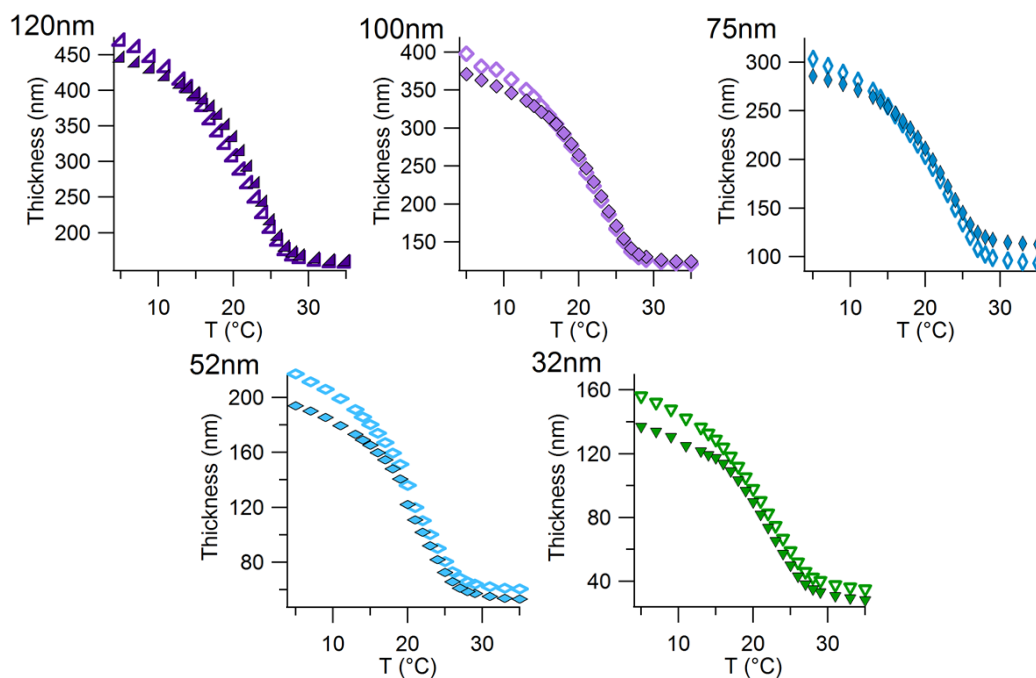


Figure S7. Comparison of swelling curves for SE and coupled water layer corrected QCM-D, where the average coupled water layer of 26 nm has been subtracted. The open symbols correspond to SE measurements and the solid symbols correspond to QCM-D measurements. The measured thickness from QCM-D and SE at temperatures greater than 18 °C is very similar except for the 75 nm film.

Part 5. Low temperature differences between QCM-D and SE

An apparent difference between the QCM-D and SE thicknesses is that the thickness difference decreases at low temperatures, especially for the thick films as shown in Figure 2. Additionally, the width of the LCST is consistent with that for the bulk when using SE data, but this is not the case for the QCM-D data (Figure 3). The unusual frequency upturn at high swelling ratios in the QCM-D data may provide some insight into this behavior. Figure S8 shows the frequency upturn for several overtones for the 32 and 120 nm films. When examining Figure S8 carefully, several salient features can be recognized. First, the reversal in the frequency (Figure S8A and S8C) occurred at the same temperature for a given overtone for both 32 nm and 120 nm (dry thickness) films and that behavior was highly reproducible. The frequency of the 9th overtone began to increase with decreasing temperature at 18 °C. Typically, an increase in frequency of a QCM is attributed to mass loss, but the SE data indicate that the film continued to swell as the temperature decreased as expected for PNIPAAm. Theoretical work based on modeling of the propagation of the shear wave through a lossy film by White and Schrag has predicted similar upturns in the frequency.⁴⁴ Future work will explore the nature of this unusual behavior. Nonetheless, this behavior illustrates care must be taken when interpreting QCM data of lossy films without secondary measurements. An increase in thickness (as determined by SE) may be accompanied by an increase in frequency (from QCM-D), which is generally considered to be indicative of a loss of adhered mass to the sensor.

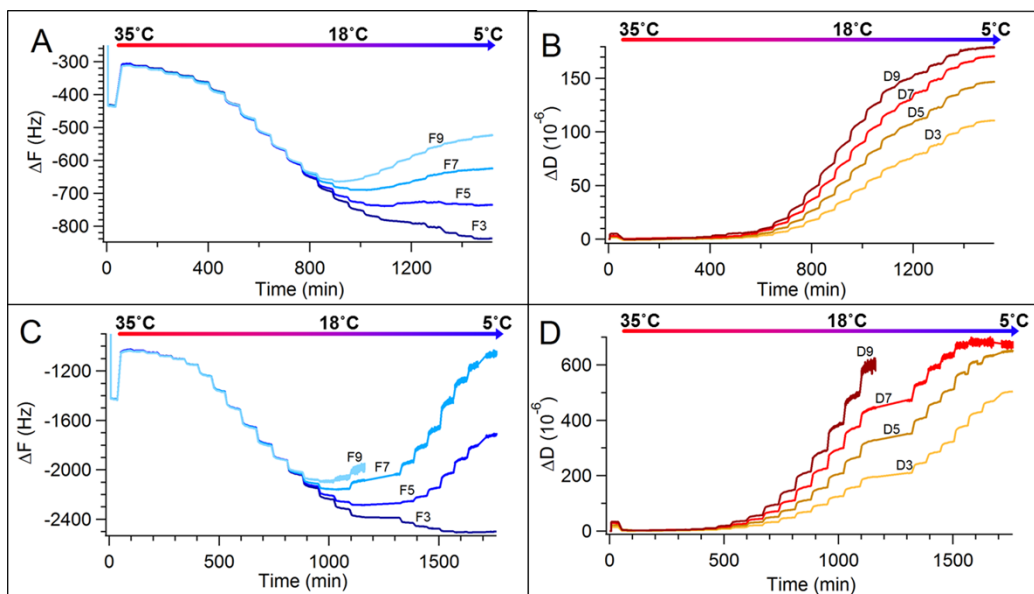


Figure S8. The frequency (F) and dissipation (D) curves from QCM-D for 3rd, 5th, 7th, and 9th overtones associated with the cooling of the 32 nm (A and B) and 120 nm films (C and D). The time is related to decreasing of the temperature from 35 °C to 5 °C. The QCM-D at low temperatures behaves in an unusual manner with an increase in both frequency and dissipation, which is atypical.

Part 6. Viscoelastic properties at high temperatures

The swelling of the NF5 film transverses regimes for QCM-D operation from rigid (Sauerbrey regime), associated with low dissipation, to highly lossy, as evidenced by the large increase in dissipation. In the low dissipation regimes, the viscoelastic properties obtained from QCM-D tend to be rather noisy as illustrated in Figure S9. In this regime, the viscoelastic properties obtained from the model depend on the initial guess and thus these values associated with the viscoelastic properties are not unique for the fits. When the film is sufficiently swollen (at a swelling ratio approaching 2.4 from an initial thickness of 100 nm), the viscosity and shear modulus obtained from the fit of the QCM-D data becomes significantly more reproducible. To explain this behavior, the operation of the QCM must be carefully considered. White and Schrag illustrated mathematically that there exists a rigid to viscoelastic transition in the operation of QCM that is dependent on the viscoelastic character and thickness of the adhered mass,⁷ which has been confirmed experimentally using swelling of a glassy polyelectrolyte film by humid air; interestingly for a 96 nm thick film, the transition from Sauerbrey to viscoelastic regime occurs at a swelling ratio of approximately 2.3.⁸ This swelling agrees with the transition where consistent viscoelastic properties are obtained for the NF5 hydrogel films from fitting the QCM-D data. This behavior suggests that the film must be sufficiently lossy to deviate from the Sauerbrey expression in order to effectively determine the viscoelastic properties of these hydrogel films.

For temperatures less than 24 °C, nearly all of the films exhibit sufficient dissipation to enable effective elucidation of the viscoelastic properties of the films (Figure 7). Figure S9 illustrates

the differences in the consistency of the fit thickness and viscoelastic properties at high temperature for a thick film. As can be clearly observed, the fit of the data is excellent across all temperatures. The film thickness for each temperature is nearly invariant with time as the ‘equilibrium’ regime is only considered here. However when considering the viscosity and shear elastic modulus determined from the same viscoelastic model over the same temperature window, the data are quite noisy, especially at low swelling extents (high temperature). Additionally, the viscosity appears to increase as the film is initially swollen, which is counter to expectations. Only for temperatures less than 24 °C is a clear understandable trend in viscosity and shear elastic modulus obtained from the viscoelastic model as denoted by the vertical dashed line in Figure S9. This behavior is consistent with the data in Figure S4 where the Sauerbrey thickness begins to deviate from the thickness obtained from the viscoelastic model in approximately this same region. In general, the dissipation increases to $\approx 10 \times 10^{-6}$ when consistent viscoelastic properties for the film are obtained from fits of the QCM-D data.

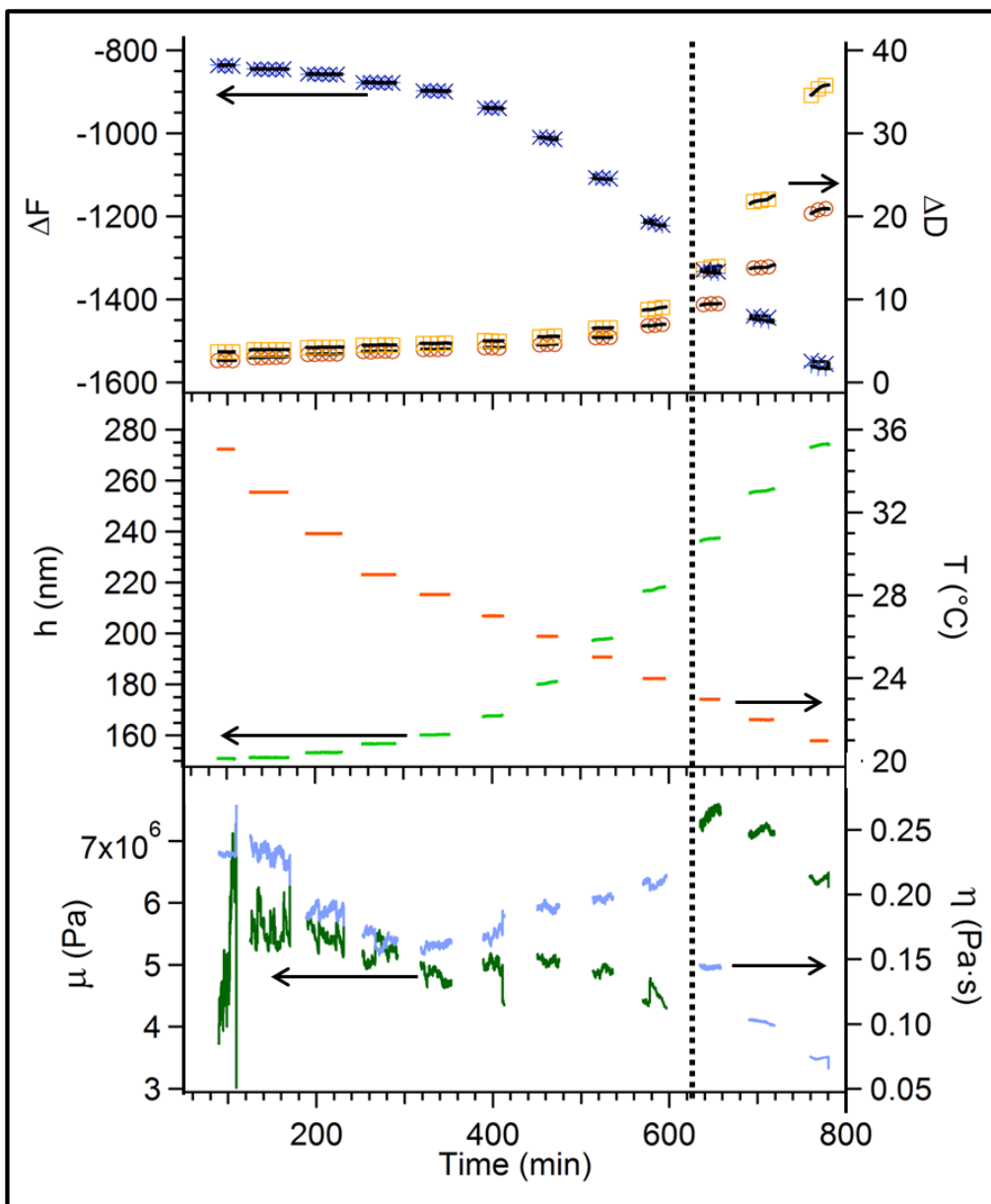


Figure S9. (top) Frequency and dissipation for F3 (×), F5 (+), D3 (○), and D5 (□) as a function of time (temperature) with fits using the viscoelastic model (solid black lines). (middle) Corresponding thickness (h , green line) from the viscoelastic model fit and associated temperature (red line). (bottom) The shear elastic modulus (μ , green) and shear viscosity (η , light blue) obtained from the fits using the viscoelastic model. Breaks in the data presented are transition regions where the film is not in equilibrium. The vertical dashed line illustrates where the fit parameters remain constant at each temperature step, which corresponds to a dissipation of approximately 10×10^{-6} .

Part 7. QCM-D overtone dependence of viscoelastic properties

In this work, the QCM-D extended viscoelastic model⁹ is used to fit the QCM-D data; this model incorporates overtone dependence in the shear elastic modulus (μ') and the shear viscosity (η_v) in the high frequency range (10^7 Hz) as:

$$\mu' = \mu'_0 (f/f_0)^{\alpha'} \quad \eta_v = \eta_{v,0} (f/f_0)^{\alpha''-1}$$

where the frequency dependent exponents are: α' (shear elastic modulus) and $\alpha''-1$ (shear viscosity). As shown in Figure S10, the frequency dependence of α' is nearly independent of film thickness for temperatures less than 20 °C, except for the thinnest film examined (10 nm). In this temperature range, α' is approximately 0.4, which illustrates that the shear elastic modulus for these hydrogels appears to be frequency dependent, even in the MHz frequency. The consistency between film thicknesses adds confidence to the physical significance of the physical properties obtained from the fits as the films all swell to similar extents and thus would be expected to have similar properties. The significant spread at higher temperatures is consistent with the prior discussion on the requirements for sufficient dissipation in order to consistently obtain viscoelastic properties for the films. One outlier is the 10 nm film where the frequency dependence becomes weaker (nearly zero). One plausible explanation is that a large fraction of chains may be bound to the surface that could also impact the elastic behavior of this thinnest film.

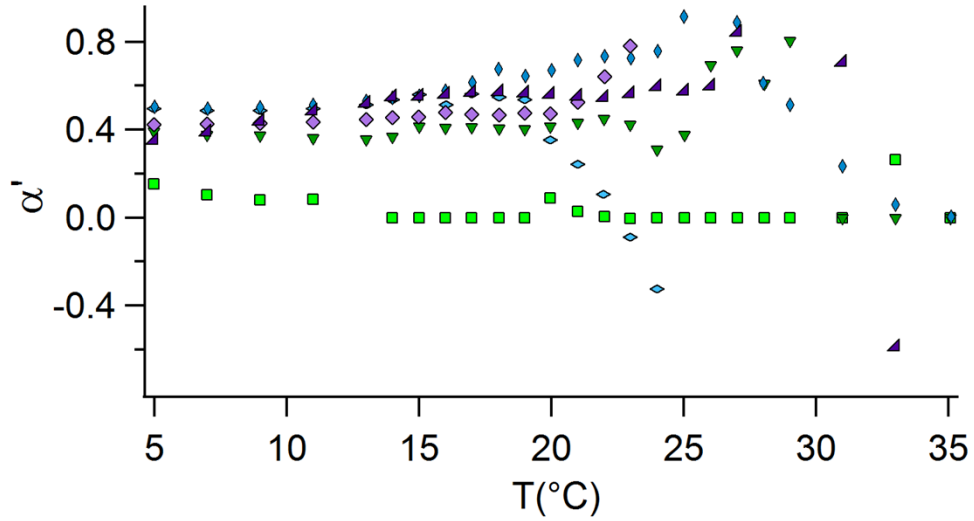


Figure S10. The frequency dependence exponent for the shear elastic modulus using the Q-Tools extended viscoelastic model for initial thickness of 10 nm (■), 32 nm (▼), 52 nm (◊), 75 nm (◊), 100 nm (◊), and 120 nm (▲). A consistent exponent of approximately 0.4 is obtained for temperatures less than 20 °C, which indicates weak frequency dependence for the shear elastic modulus in the MHz regime. One outlier is the 10 nm film with no apparent dependence on frequency for the shear elastic modulus.

Similarly, Figure S11 illustrates the frequency dependence of $\alpha''-1$, which is associated with the shear viscosity. Again, the behavior is similar for all films except for the thinnest (10 nm) film. Unlike the shear elastic modulus, the shear viscous modulus is frequency independent (Figure S11). This suggests that the hydrogel is in the terminal regime in the MHz frequency regime as would be expected. Interestingly, $\alpha''-1$ is negative for the 10 nm film with an average dependence around -1.2. This suggests shear thickening for the hydrogel when chains are predominately attached to the rigid substrate.

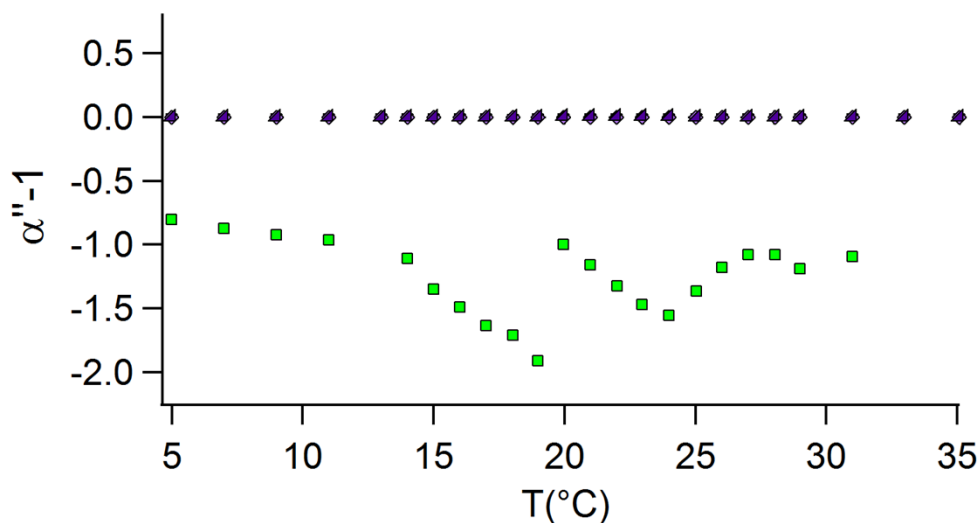


Figure S11. The frequency dependent exponent for the shear viscosity using Q-Tools extended viscoelastic model for initial film thicknesses of 10nm (■), 32nm (▼), 52nm (◆), 75nm (◆), 100nm (◆), and 120nm (◆). The exponent is consistently near zero for all of the films except the 10 nm film. This suggests no dependence on frequency for the shear viscosity for the thicker films.

REFERENCES

1. K. K. Kanazawa and J. G. Gordon, *Anal. Chim. Acta*, 1985, **175**, 99-105.
2. P. J. Linstrom, W. G. Mallard and Eds, *NIST Chemistry WebBook, NIST Standard Reference Database*, <http://webbook.nist.gov> edn., National Institute of Standards and Technology, Gaithersburg MD, 20899, 2013.
3. G. Sauerbrey, *Z. Phys.*, 1959, **155**, 206-222.
4. J. Tian, T. A. P. Seery and R. A. Weiss, *Macromolecules*, 2004, **37**, 9994-10000.
5. M. E. Harmon, T. A. M. Jakob, W. Knoll and C. W. Frank, *Macromolecules*, 2002, **35**, 5999-6004.
6. F. Hook, B. Kasemo, T. Nylander, C. Fant, K. Sott and H. Elwing, *Anal. Chem.*, 2001, **73**, 5796-5804.
7. C. C. White and J. L. Schrag, *J. Chem. Phys.*, 1999, **111**, 11192-11206.
8. B. D. Vogt, E. K. Lin, W. L. Wu and C. C. White, *J. Phys. Chem. B*, 2004, **108**, 12685-12690.
9. N. B. Eisele, F. I. Andersson, S. Frey and R. P. Richter, *Biomacromolecules*, 2012, **13**, 2322-2332.